Int J Clin Exp Pathol 2017;10(1):148-155
www.ijcep.com /ISSN:1936-2625/IJCEP0042227

Original Article

Molecular MRI of activated hepatic stellate cells in rats with early stage of liver fibrosis by targeting hepatic integrin α5β1

Wei Zhang[1], Qi-Yuan Wang[2], Guo-Hua Fan[1]

[1]*Department of Radiology, The Second Affiliated Hospital of Soochow University, Suzhou, Jiangsu Province, China;* [2]*Department of Radiology, Second Affiliated Hospital, Zhejiang University College of Medicine, Hangzhou, Zhejiang Province, China*

Received October 18, 2016; Accepted October 26, 2016; Epub January 1, 2017; Published January 15, 2017

Abstract: Objective: To investigate the feasibility of ultrasmall superparamagnetic iron oxide (USPIO) modified by anti-α5β1 integrin monoclonal antibody (mAb) for targeting activated hepatic stellate cells (HSCs) in early stage of hepatic fibrosis rats in vivo. Methods: The early stage hepatic fibrosis model of rats was established by injecting carbon tetrachloride subcutaneously. The anti-α5β1 integrin mAb-USPIO probe was prepared by conjugating anti-α5β1 integrin mAb with USPIO through carbodiimide method. Four normal rats were treated with anti-α5β1 integrin mAb-USPIO as control group. Twelve hepatic fibrosis rats were divided randomly into three groups and then were treated with anti-α5β1 integrin mAb-USPIO, naked USPIO and anti-α5β1 integrin mAb respectively. Abdominal magnetic resonance imaging (MRI) was performed for all rats before and 4 h after administration of the probes. The liver: muscle contrast-to-noise ratio (CNR) of the rats in all 4 groups before and 4 h after probe injection was calculated and analyzed. Liver tissue was subjected to pathologic scoring of fibrosis and location of iron particles of probes in normal and fibrosis rats was also observed. Results: The liver: muscle CNR 4 h after probes injection in hepatic fibrosis rats treated with anti-α5β1 integrin mAb-USPIO was much higher than that in normal rats treated with anti-α5β1 integrin mAb-USPIO and fibrosis rats treated with naked USPIO ($P<0.01$). Prussian blue staining and transmission electron microscopy demonstrated that the anti-α5β1 integrin mAb-USPIO probe was specifically engulfed by the activated HSCs in fibrosis rats. Conclusion: In vivo molecular MRI of activated HSCs in early stage of hepatic fibrosis rats was feasible by targeting α5β1 integrin with anti-α5β1 integrin mAb-USPIO probe.

Keywords: Molecular imaging, magnetic resonance imaging, liver fibrosis, hepatic stellate cell, integrin α5β1, ultrasmall superparamagnetic iron oxide

Introduction

With the increasing trend of aging population, chronic liver disease tends to be a severe global health problem. Long-lasting chronic liver injury is likely to lead to liver fibrosis which is characterized by different etiologic forms of chronic liver disease such as hepatitis B or C, non-alcoholic steatohepatitis and so on [1]. Liver fibrosis can be treated due to its reversibility to some extent [2]. Only if diagnosed in early stage and measures be taken promptly, liver impairment in hepatic fibrosis is most likely to resume normal structure and function. On the contrary, liver fibrosis may eventually lead to cirrhosis, the final stage of the disease which may result in a series of complications including refractory ascites, digestive tract bleeding, hepatocellular carcinoma, etc. [3]. Pathological diagnosis by percutaneous liver biopsy has been considered as the gold standard for assessing fibrosis progression, but it is an invasive procedure during which patient compliance and potential complications is a great concern [4]. In addition, clinical application of liver biopsy is partly limited by sampling error and interobserver variation [5]. Serum markers of liver fibrosis are relatively unreliable because of the low sensitivity and specificity [6]. Conventional imaging techniques, including US [7], CT [8] and MR imaging [9] have played an important role in evaluating advanced hepatic

fibrosis and cirrhosis. Nevertheless, they are incapable for detecting early stage of liver fibrosis. More recently, transient elastography [10], magnetic resonance elastography (MRE) [11, 12] and magnetic resonance spectroscopy (MRS) [13, 14] have been studied for their role in staging liver fibrosis, but these techniques are still in their infancy for widespread use clinically. Therefore, a novel strategy is in urgent need which is both noninvasive and reliable for the diagnosis of the early stage of liver fibrosis.

Liver fibrosis is characterized by an extensive accumulation of the extracellular matrix (ECM) and failure to degrade it [1]. The hepatic stellate cells (HSCs), undergoing the transformation from quiescent to activated phenotype called the myofibroblast-like cells when liver damage occurs, are the main source of ECM materials [15]. Thus, HSCs play a fundamental role in the development of liver fibrosis. Over the past decades, HSCs have been studied not only as a prognostic indicator of progression of liver fibrosis but also as an attractive target for antifibrotic therapies due to their pivotal role in the evolution of liver fibrosis [16, 17]. Integrins are a large family of cell surface receptors and are consisted of α and β subunits, which can interact with other cell adhesion molecules and ECM components, and mediate the cell-cell and cell-matrix adhesions. The integrin-mediated adhesions could promote activation, proliferation, differentiation and survival of the HSCs in the process of liver fibrosis [18]. In addition, the expression of integrin α5β1, the fibronectin receptor, was remarkably increased on activated HSCs stimulated by transforming growth factor-β1 (TGF-β1) in fibrotic livers [19]. Furthermore, integrin α5β1 has been reported in the fibrosis of some other organs and tumor target therapy [20]. However, to the best of our knowledge, there is no correlation study regarding the molecular imaging of liver fibrosis using integrin α5β1 as a target.

In recently years, molecular imaging, which is committed to image cell or molecule in the physiological and pathological process in vivo, has been successfully applied in diagnosing tumor, cardiovascular diseases, etc. and monitoring the effect of treatment with the help of SPECT [21], PET [22], MRI [23] and contrast-enhanced Ultrasonography [24]. Although, molecular imaging possesses the advantage as novel noninvasive method for certain diseases, the key problem remains in how to find a specific biomarker for molecular probe.

In the present study, we prepared anti-α5β1 integrin mAb-USPIO and explored whether this probe could specifically bind to integrin α5β1 expressed on the surface of the activated HSCs in early stage of liver fibrosis.

Materials and methods

Animals

Sixteen seven-week-old male Sprague-Dawley rats (200-220 g) were purchased from Shanghai Slac Laboratory Animal Co. Ltd (Shanghai, China) and fed on standard laboratory rat chow under 12-hour dark/light cycles. This experiment was performed in accordance with the National Institute of Health Policy on the Care and Use of Laboratory Animals and approved by the Ethics Committee of the Second Affiliated Hospital of Soochow University.

Animal model of liver fibrosis

In order to induce liver fibrosis, twelve normal rats were injected subcutaneously with 3 mL/kg of 40% carbon tetrachloride (CCl_4) oil solution twice a week for 3 weeks. Four normal rats treated with only pure olive oil served as a control group. All rats were sacrificed immediately after the final MRI scanning.

Synthesis of the anti-α5β1 integrin mAb-USPIO probe

The anti-α5β1 integrin monoclonal antibody (mAb) was purchased from Bioss Inc (Woburn, MA, USA). USPIO (20 nm, surface: COOH) was purchased from Micromod Partikeltechnologie GmbH (Rostock, Germany). The conjugation method of anti-α5β1 integrin mAb to USPIO is based on the carbodiimide/N-hydroxysuccinimide (NHS) activation of the carboxylic acid groups on USPIO surfaces followed by reaction with amino groups of the anti-α5β1 integrin mAb, which leads to a random amide bond formation between them [25] (**Figure 1**). The specific synthesis procedure was operated by Zoonbio Biotechnology Co. Ltd. (Nanjing, Jiangsu, China), who supplied all chemical reagents and devices needed during conjugation.

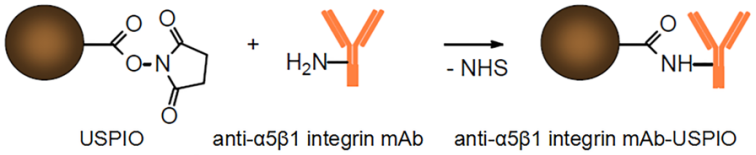

Figure 1. Synthetic illustration of the specific probe. The carboxylic acid groups on USPIO surfaces react with amino groups of the anti-α5β1 integrin mAb, forming a random amide bond formation between them.

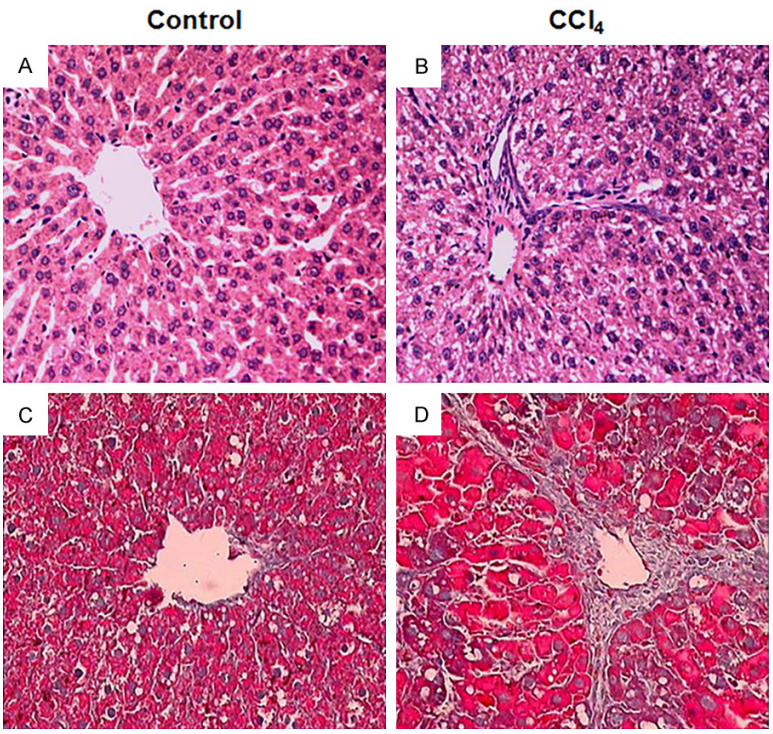

Figure 2. Characterization of fibrosis in the animal model. H&E staining (A, B) reveals small amount of fibrotic expansions in portal area in the rat injured by CCl_4 corresponding to early stage of liver fibrosis (Ishak 1) (B, ×200). No detectable fibrosis is found in the control sample (A, ×200). Masson's trichrome staining (C, D) shows more portal fibrotic expansions and some short fibrous septum in the CCl_4-treated rat (Ishak 2) (D, ×200). The control sample is normal without fibrosis (C, ×200).

MR imaging protocol

The twelve fibrosis rats were divided randomly into three groups. One group was given anti-α5β1 integrin mAb-conjugated USPIO while the other two groups and four normal rats were given naked USPIO, anti-α5β1 integrin mAb and anti-α5β1 integrin mAb-USPIO respectively for control purpose. MR imaging was performed on a clinical 1.5-T MR scanner (Philips Achieva System, Holland) three days after the final CCl_4 injection to avoid acute effects, with the rats in prone decubitus and Micro-47 coil wrapped around their abdomen. The rats were scanned using a gradient-echo sequence (FFE T2WI) with an echo time of 12 ms and a repetition time of 544 ms. Additional parameters were as follows: slice thickness, 3 mm; field of view, 60×60 mm^2; and matrix, 256×256. MR images were obtained before and 4 h after the injection of molecular probes via femoral vein catheter at an iron dose of 100 μmol/kg body weight.

Image analysis

Regions of interest, excluding the major vessels and artifacts, were drawn on the liver parenchyma and adjacent dorsal muscle on the MR image for measuring the signal intensity (SI). Noise of the background was estimated from the standard deviation (SD) of SI in the air adjacent to the rats. Contrast-to-noise ratio (CNR) was calculated as $\{(SI_{liver} - SI_{muscle})/SD_{air}\}$. The software of ViewForum 4.1 (Philips, Holland) was employed for measuring the MR SI.

Histopathological examinations and detection of iron nanoparticles in the HSCs in liver of rats

The rats were sacrificed with deep anesthesia (3.6% chloral hydrate, 1 ml/100 g body weight, intraperitoneally). The liver collected from the rats after MRI scanning was divided into several lumps according to the examinations introduced below. The histopathological examinations were performed with Hematoxylin-eosin and Masson's trichrome staining using standard staining protocol to score the amount of liver disease according to the method of

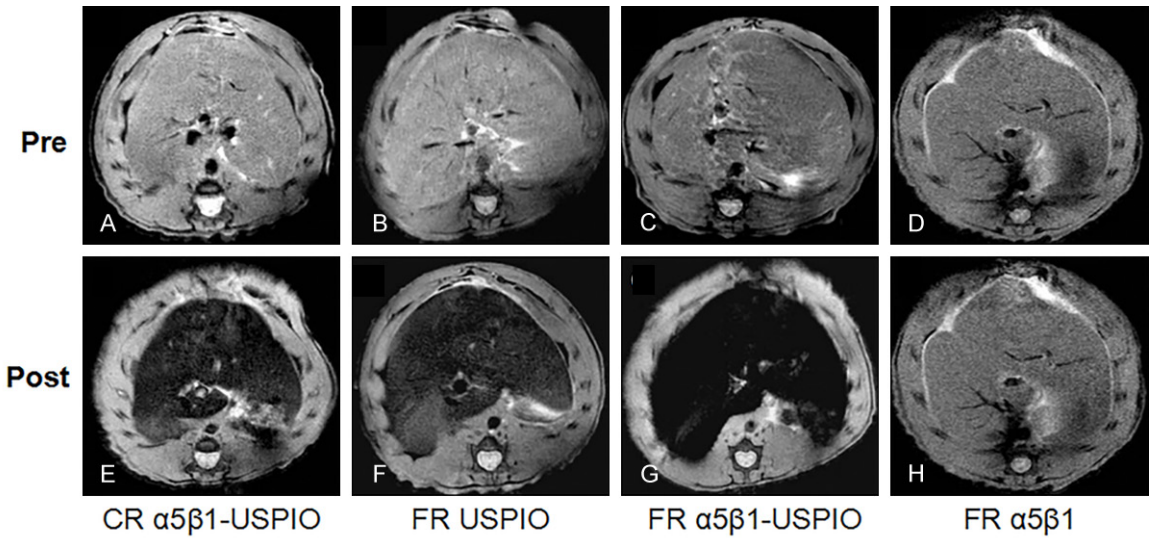

Figure 3. MR imaging of liver in control rats and fibrosis rats before and 4 h after injection of specific probes. The signal intensity (SI) of liver in all four groups is similar before injection of probes (A-D). Four hours after injection of probes, signal decrease of entire liver was apparently visualized in the group of control rats treated with α5β1-USPIO (E) and fibrosis rats treated with USPIO (F). More significant reduction of the SI of the liver is observed in the group of fibrosis rats treated with α5β1-USPIO (G). There is no obvious change of the SI of liver in the group of fibrosis rats treated with anti-α5β1 integrin mAb (H). CR and FR are short for control rats and fibrosis rats respectively.

Table 1. The liver: muscle CNR of four groups of rats comparing pre and post administration of probes by paired-samples *t*-test

Groups	Pre-injection	Post-injection	*t* value	*p* value
CR α5β1-USPIO	45.37±1.87	175.51±12.49	26.65	0
FR α5β1-USPIO	44.63±1.61	255.74±18.3	30.32	0
FR USPIO	44.56±2.08	157.96±13.72	20.38	0
FR α5β1	44.82±1.39	45.46±8.24	1.45	0.24

CR and FR are short for control rats and fibrosis rats respectively.

Ishak fibrosis score [26]. Prussian blue staining and transmission electron microscopy (TEM, Hitachi H-600, Tokyo, Japan) examination were performed according to standard procedures for detecting iron particles of the probe in the liver of rats. A board certified liver pathologist reviewed all slides blindly.

Statistical analysis

All collected data were expressed as mean ± SD. Statistical analysis was carried out with SPSS 17.0 statistical software (Chicago, IL, USA). The CNR before and 4 h after administration of the probes inside each group was compared using paired-samples *t*-test. Comparisons of the CNR between groups were fulfilled by one-way analysis of variance (ANOVA) followed by Student-Newman-Keuls (SNK) test. $P<0.05$ was considered statistically significant.

Results

Characterization of animal model

After treatment with 40% CCl_4 in rats for 3 weeks, early stage of liver fibrosis was established: five rats with an Ishak score of 1 (**Figure 2B**) and seven rats with an Ishak score of 2 (**Figure 2D**). No detectable fibrosis in the control rats was found (Ishak score 0, **Figure 2A**, **2C**).

Molecular MR imaging of activated HSCs in early stage of liver fibrosis

The SI of liver of four groups of rats was similar on unenhanced MR images (**Figure 3A-D**). After injection of contrast agents, signal decrease of entire liver was apparently visualized in the group of control rats treated with anti-α5β1 integrin mAb-USPIO (α5β1-USPIO) (**Figure 3E**) and group of fibrosis rats treated with naked USPIO (**Figure 3F**). Significant reduction of the SI of the liver was observed in the group of fibrosis rats treated with α5β1-USPIO (**Figure 3G**). However, no obvious change of the SI of liver was found in the group of fibrosis rats

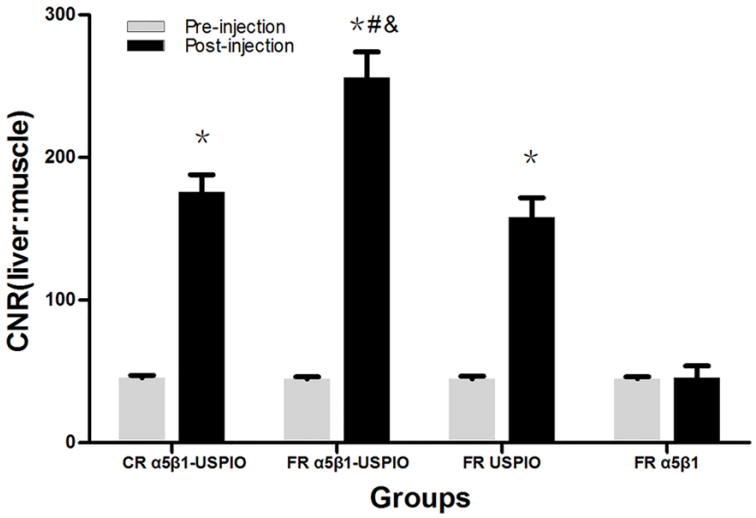

Figure 4. The liver: muscle CNR of four groups of rats pre and post administration of probes. The pre-injection liver: muscle CNR of probes has no obvious statistical difference among all four groups of rats (F=0.306, P=0.820) by one-way ANOVA. The liver: muscle CNR of probes 4 h after injection has no significant statistical difference between control rats treated with α5β1-USPIO and fibrosis rats treated with USPIO (P=0.094); Significant statistical difference (P<0.01) among all the other groups are detected when compared with one another by the SNK method. *P<0.01 versus pre-injection, #P<0.01 versus CR α5β1-USPIO group, &P<0.01 versus FR USPIO group. CR and FR are short for control rats and fibrosis rats respectively.

treated with anti-α5β1 integrin mAb (**Figure 3H**).

The liver: muscle CNR of four groups of rats was shown in **Table 1**. There were significant differences between the liver: muscle CNR before injection and that 4 h after injection in three other groups of rats (P<0.01) except the group of fibrosis rats treated with anti-α5β1 integrin mAb (P=0.24). The liver: muscle CNR 4 h after injection of probes had no significant statistic difference between control rats treated with α5β1-USPIO and fibrosis rats treated with USPIO (P=0.094), while there were significant differences between all the other groups (P<0.01) when they were multi-compared with each other by the SNK method (**Figure 4**).

Distribution of iron nanoparticles of probes in the liver

By Prussian blue staining, the location of iron nanoparticles of probes in the control rats (**Figure 5A**) and fibrosis rats (**Figure 5B**) treated with USPIO was similar, mainly situated in the blood sinusoid in the liver in consistent with the location of the Kupffer cells. The iron nanoparticles in the fibrosis rats treated with α5β1-USPIO (**Figure 5C**) were found distributing more intensively in the perisinusoidal space of Disse in accord with where HSCs was located. TEM proved that there was massive iron nanoparticles in the lysosomes inside the HSCs in the fibrosis rats treated with α5β1-USPIO (**Figure 6A**). In contrast, the lysosomes, containing iron nanoparticles, were not found in the HSCs in the control rats (**Figure 6B**) and fibrosis rats treated with USPIO (**Figure 6C**).

Discussion

To the best of our knowledge, this is the first report of the molecular MR imaging of activated HSCs in rats with early stage of liver fibrosis by targeting hepatic integrin α5β1 in vivo. The histopathological examinations demonstrated that all the fibrosis rats were in the early stage of liver fibrosis according to the criteria of Ishak. We observed that decrease of SI of the entire liver was the most pronounced by treated with anti-α5β1 integrin mAb-USPIO than with naked USPIO in hepatic fibrosis rats and with anti-α5β1 integrin mAb-USPIO in control rats. Furthermore, the activated HSCs in early stage of liver fibrosis could engulf iron nanoparticles of the probe specifically. These findings indicate that molecular targeting imaging of activated HSCs in liver fibrosis can be realized in vivo using MRI via a specific probe.

MRI has played an important role in the diagnosis and staging of liver fibrosis because of its non-invasive, non-ionizing radiation and high spatial resolution. Conventional MRI [9, 27] and double-contrast MRI [28] have been widely applied to evaluate liver fibrosis, but the sensitivity and specificity remain low. Functional MRI, including MRE [29], MRS [30], diffusion tensor imaging (DTI) [31] and perfusion weighted MR imaging (PWI) [32], has shown promising role in detecting fibrosis. However, the parameters used in these methods are non-specific

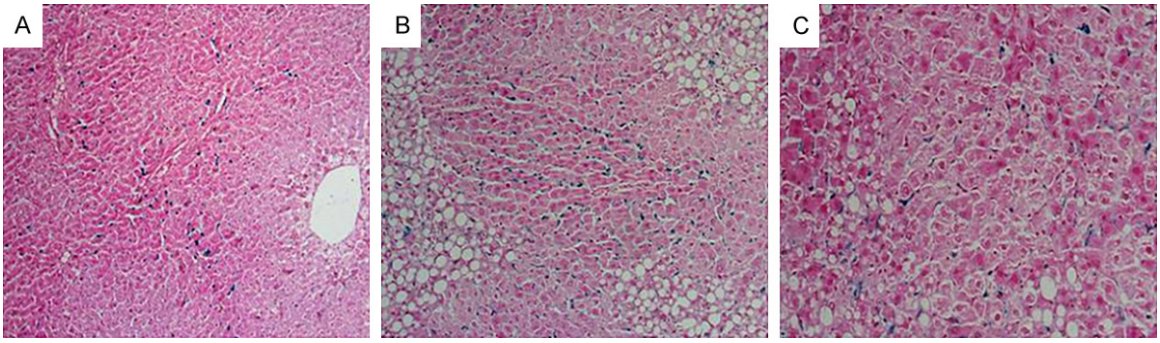

Figure 5. Prussian blue staining of liver tissue after administration of probes. The location of blue stained iron particles of probes in control rats (A, ×100) and fibrosis rats (B, ×100) treated with USPIO is similar, mainly situated in the blood sinusoid in the liver. However, the iron particles in the fibrosis rats treated with α5β1-USPIO (C, ×200) are distributed more intensively in the perisinusoidal space of Disse where the HSCs locate.

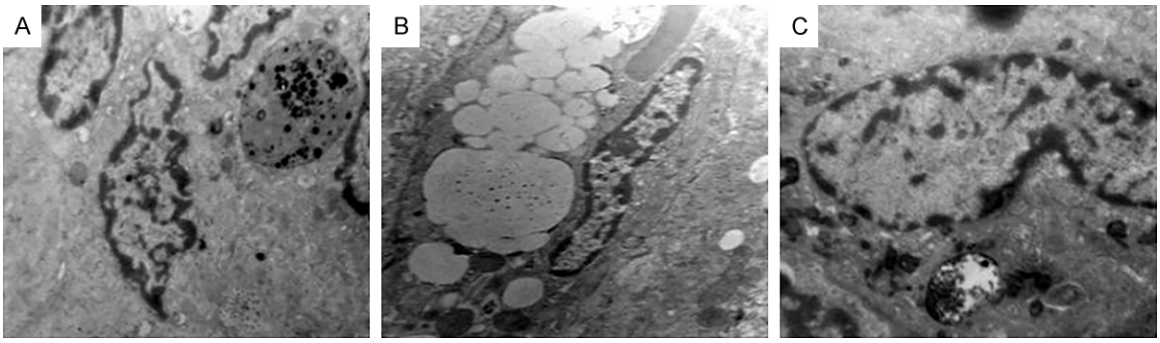

Figure 6. Transmission electron microscopy (TEM) of hepatic stellate cell (HSC) in liver tissue after administration of probes. TEM shows that there are massive iron nanoparticles in the lysosomes inside the HSC in the fibrosis rats treated with α5β1-USPIO (A, ×8000). In contrast, the lysosomes, containing iron nanoparticles, are not found in the HSC in the control rats (B, ×10000) and fibrosis rats treated with USPIO (C, ×10000).

for liver fibrosis and are easily affected by factors such as inflammation, ascites, and liver perfusion. The molecular MRI may be complementary to these above-mentioned MRI techniques and in fact has been tentatively applied in assessing liver fibrosis [33]. Unfortunately, the research on molecular MRI of liver fibrosis is scant up till now. The main reason is that it is difficult to find the biomarker of liver fibrosis and then to synthesize the corresponding targeted probe.

In our study, we prepared anti-α5β1 integrin mAb-conjugated USPIO as the specific probe to target the activated HSCs in rats with early stage of liver fibrosis by combining integrin α5β1 on the surface of the activated HSCs. We then performed MRI for all rats by applying anti-α5β1 integrin mAb-conjugated USPIO, naked USPIO and anti-α5β1 integrin mAb to fibrosis rats as well as applying anti-α5β1 integrin mAb-conjugated USPIO to normal rats. We found that the decrease of SI of the entire liver was similar in normal rats treated with anti-α5β1 integrin mAb-conjugated USPIO (**Figure 3E**) and fibrosis rats treated with naked USPIO (**Figure 3F**); significant reduction was observed in the group of fibrosis rats treated with anti-α5β1 integrin mAb-USPIO (**Figure 3G**); but there was no obvious change in the group of fibrosis rats treated with anti-α5β1 integrin mAb (**Figure 3H**). We speculate that the iron particles which could cause the decrease of T2 SI of liver could be only devoured by the Kupffer cells in both normal rats treated with anti-α5β1 integrin mAb-conjugated USPIO (**Figure 5A**) and fibrosis rats treated with USPIO (**Figure 5B**). However, the activated HSCs could specifically engulf the iron particles in fibrosis rats treated with anti-α5β1 integrin mAb-conjugated USPIO by taking anti-α5β1 integrin mAb as the ligand for integrin α5β1 receptor. So the iron particles could

be taken up not only by the Kupffer cells (**Figure 5C**) but also mostly by the activated HSCs (**Figure 6A**) in fibrosis rats. As a result, there was more increase of liver: muscle CNR in hepatic fibrosis rats group treated with anti-α5β1 integrin mAb-conjugated USPIO after injection of probes than that in normal rats treated with anti-α5β1 integrin mAb-USPIO and fibrosis rats treated with naked USPIO (**Table 1**).

Our study has several limitations. Firstly, there may be some differences in rat liver fibrosis model induced by CCl_4 compared with human hepatic fibrosis caused by different etiology. Most notably, repeated administration of CCl_4 in rats will induce liver fibrosis within a few weeks, whereas patients with liver disease may take several years in the development of liver fibrosis. Secondly, we did not illustrate the correlation between the amount of iron particles engulfed by activated HSCs and stages of liver fibrosis. So, the relationship between amount of iron particles uptake by activated HSCs and the related reduction of signal intensity of the liver in different pathological stages of liver fibrosis needs to be further studied. Thirdly, we did not take any anti-fibrotic modalities for liver fibrosis, thus the efficacy of this specific MR molecular probe in monitoring of therapeutic effects in fibrosis cannot be evaluated.

In conclusion, our study has shown that it is feasible to achieve the specific targeted imaging of activated HSCs in early stage of liver fibrosis in vivo using the specific molecular probe targeting integrin α5β1. This method can be used in diagnosing liver fibrosis in early stage, however, its role in monitoring antifibrogenetic therapeutic effects remains to be further studied.

Acknowledgements

This study was supported by Suzhou Science and Technology Development Planning Foundation (Grant No. SYS201474).

Disclosure of conflict of interest

None.

Address correspondence to: Dr. Guo-Hua Fan, Department of Radiology, The Second Affiliated Hospital of Soochow University, 1055 Sanxiang Road, Suzhou 215004, Jiangsu Province, China. Tel: +86-512-67783830; Fax: +86-512-68284303; E-mail: fangh22@126.com

References

[1] Wallace K, Burt AD, Wright MC. Liver fibrosis. Biochem J 2008; 411: 1-18.
[2] Atta HM. Reversibility and heritability of liver fibrosis: implications for research and therapy. World J Gastroenterol 2015; 21: 5138-5148.
[3] Li G, Cai G, Li D, Yin W. MicroRNAs and liver disease: viral hepatitis, liver fibrosis and hepatocellular carcinoma. Postgrad Med J 2014; 90: 106-112.
[4] Fern Ndez-Salazar L, Velayos B, Aller RO, Lozano FL, Garrote JA, Gonz Lez JM. Percutaneous liver biopsy: patient's point of view. Scand J Gastroenterol 2011; 46: 727-731.
[5] Rockey DC, Caldwell SH, Goodman ZD, Nelson RC, Smith AD; American Association for the Study of Liver Diseases. Liver biopsy. Hepatology 2009; 49: 1017-1044.
[6] Castera L. Hepatitis B: are non-invasive markers of liver fibrosis reliable? Liver Int 2014; 34: 91-96.
[7] Mueller-Abt PR, Frawley KJ, Greer RM, Lewindon PJ. Comparision of ultrasound and biopsy findings in children with cystic fibrosis ralated liver disease. J Cyst Fibros 2008; 7: 215-221.
[8] Huber A, Ebner L, Montani M, Semmo N, Roy Choudhury K, Heverhagen J, Christe A. Computed tomography findings in liver fibrosis and cirrhosis. Swiss Med Wkly 2014; 144: w13923.
[9] Aubé C, Moal F, Oberti F, Roux J, Croquet V, Gallois Y, Argaud C, Caron C, Calès P. Diagnosis and measurement of liver fibrosis by MRI in bile duct ligated rats. Dig Dis Sci 2007; 52: 2601-2609.
[10] Thiele M, Detlefsen S, Sevelsted Møller L, Madsen BS, Fuglsang Hansen J, Fialla AD, Trebicka J, Krag A. Transient and 2-dimensional shear-wave elastography provide comparable assessment of alcoholic liver fibrosis and cirrhosis. Gastroenterology 2016; 150: 123-133.
[11] Chang W, Lee JM, Yoon JH, Han JK, Choi BI, Yoon JH, Lee KB, Lee KW, Yi NJ, Suh KS. Liver fibrosis staging with MR elastography: comparison of diagnostic performance between patients with chronic hepatitis B and those with other etiologic causes. Radiology 2016; 280: 88-97.
[12] Shi Y, Xia F, Li QJ, Li JH, Yu B, Li Y, An H, Glaser KJ, Tao S, Ehman RL, Guo QY. Magnetic resonance elastography for the evaluation of liver fibrosis in chronic hepatitis B and C by using both gradient-recalled echo and spin-echo echo planar imaging: a prospective

study. Am J Gastroenterol 2016; 111: 823-833.
[13] Godfrey EM, Patterson AJ, Priest AN, Davies SE, Joubert I, Krishnan AS, Griffin N, Shaw AS, Alexander GJ, Allison ME, Griffiths WJ, Gimson AE, Lomas DJ. A comparison of MR elastography and (31)P MR spectroscopy with histological staging of liver fibrosis. Eur Radiol 2012; 22: 2790-2797.
[14] Embade N, Mariño Z, Diercks T, Cano A, Lens S, Cabrera D, Navasa M, Falcón-Pérez JM, Caballería J, Castro A, Bosch J, Mato JM, Millet O. Metabolic characterization of advanced liver fibrosis in HCV patients as studied by serum 1H-NMR spectroscopy. PLoS One 2016; 11: e0155094.
[15] Mallat A, Lotersztajn S. Reversion of hepatic stellate cell to a quiescent phenotype: From myth to reality? J Hepatol 2013; 59: 383-386.
[16] Tan Z, Qian X, Jiang R, Liu Q, Wang Y, Chen C, Wang X, Ryffel B, Sun B. IL-17A plays a critical role in the pathogenesis of liver fibrosis through hepatic stellate cell activation. J Immunol 2013; 191: 1835-1844.
[17] Narmada BC, Kang Y, Venkatraman L, Peng Q, Sakban RB, Nugraha B, Jiang X, Bunte RM, So PT, Tucker-Kellogg L, Mao HQ, Yu H. Hepatic stellate cell-targeted delivery of hepatocyte growth factor transgene via bile duct infusion enhances its expression at fibrotic foci to regress dimethylnitrosamine-induced liver fibrosis. Hum Gene Ther 2013; 24: 508-519.
[18] Patsenker E, Stickel F. Role of integrins in fibrosing liver diseases. Am J Physiol Gastrointest Liver Physiol 2011; 301: G425-G434.
[19] Zhou X, Zhang Y, Zhang J, Zhu H, Zhou X, Du W, Zhang X, Chen Q. Expression of fibronectin receptor, integrin alpha 5 beta 1 of hepatic stellate cells in rat liver fibrosis. Chin Med J (Engl) 2000; 113: 272-276.
[20] Gooz P, Dang Y, Higashiyama S, Twal WO, Haycraft CJ, Gooz M. A disintegrin and metalloenzyme (ADAM) 17 activation is regulated by α5β1 integrin in kidney mesangial cells. PLoS One 2012; 7: e33350.
[21] Palumbo B, Buresta T, Nuvoli S, Spanu A, Schillaci O, Fravolini ML, Palumbo I. SPECT and PET serve as molecular imaging techniques and in vivo biomarkers for brain metastases. Int J Mol Sci 2014; 15: 9878-9893.
[22] Dissoki S, Abourbeh G, Salnikov O, Mishani E, Jacobson O. PET molecular imaging of angiogenesis with a multiple tyrosine kinase receptor-targeted agent in a rat model of myocardial infarction. Mol Imaging Biol 2015; 17: 222-230.
[23] Pernia Leal M, Rivera-Fernández S, Franco JM, Pozo D, de la Fuente JM, García-Martín ML. Long-circulating PEGylated manganese ferrite nanoparticles for MRI-based molecular imaging. Nanoscale 2015; 7: 2050-2059.
[24] Streeter JE, Gessner RC, Tsuruta J, Feingold S, Dayton PA. Assessment of molecular imaging of angiogenesis with three-dimensional ultrasonography. Mol Imaging 2011; 10: 460-468.
[25] Grabarek Z, Gergely J. Zero-length crosslinking procedure with the use of active esters. Anal Biochem 1990; 185: 131-135.
[26] Ishak K, Baptista A, Bianchi L, Callea F, De Groote J, Gudat F, Denk H, Desmet V, Korb G, MacSween RN. Histological grading and staging of chronic hepatitis. J Hepatol 1995; 22: 696-699.
[27] Aubé C, Moal F, Oberti F, Roux J, Croquet V, Gallois Y, Argaud C, Caron C, Calès P. Diagnosis and measurement of liver fibrosis by MRI in bile duct ligated rats. Dig Dis Sci 2007; 52: 2601-2609.
[28] Aguirre DA, Behling CA, Alpert E, Hassanein TI, Sirlin CB. Liver fibrosis: noninvasive diagnosis with double contrast material-enhanced MR imaging. Radiology 2006; 239: 425-437.
[29] Venkatesh SK, Xu S, Tai D, Yu H, Wee A. Correlation of MR elastography with morphometric quantification of liver fibrosis (Fibro-C-Index) in chronic hepatitis B. Magn Reson Med 2014; 72: 1123-1129.
[30] Cheung JS, Fan SJ, Gao DS, Chow AM, Yang J, Man K, Wu EX. In vivo lipid profiling using proton magnetic resonance spectroscopy in an experimental liver fibrosis model. Acad Radiol 2011; 18: 377-383.
[31] Cheung JS, Fan SJ, Gao DS, Chow AM, Man K, Wu EX. Diffusion tensor imaging of liver fibrosis in an experimental model. J Magn Reson Imaging 2010; 32: 1141-1148.
[32] Leporq B, Dumortier J, Pilleul F, Beuf O. 3D-liver perfusion MRI with the MS-325 blood pool agent: a noninvasive protocol to asses liver fibrosis. J Magn Reson Imaging 2012; 35: 1380-1387.
[33] Ehling J, Bartneck M, Fech V, Butzbach B, Cesati R, Botnar R, Lammers T, Tacke F. Elastin-based molecular MRI of liver fibrosis. Hepatology 2013; 58: 1517-1518.